

Oxidative Coupling Mechanisms: Current State of Understanding

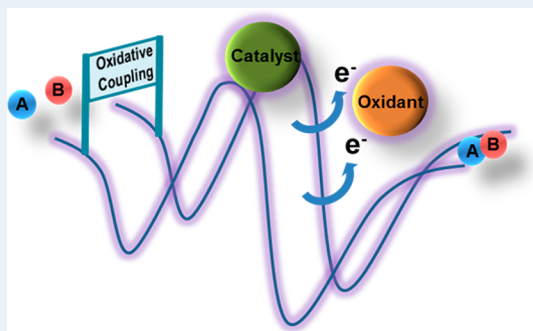
Ignacio Funes-Ardoiz[†] and Feliu Maseras^{*,†,‡}

[†]Institute of Chemical Research of Catalonia (ICIQ), The Barcelona Institute of Science and Technology, Avda. Paisos Catalans, 16, 43007 Tarragona, Catalonia, Spain

[‡]Departament de Química, Universitat Autònoma de Barcelona, 08193 Bellaterra, Catalonia, Spain

ABSTRACT: Oxidative coupling reactions, where two electrons are released from the reactants and trapped by an oxidant, have arisen as a versatile alternative to cross-coupling in chemical synthesis. Despite the large number of experimental reports on the process, a clear mechanistic picture is only starting to emerge. In this perspective, we highlight the contribution from density functional theory (DFT) calculations to the computational characterization of this mechanism. Oxidative coupling processes have been reported, differing in both the catalyst (radicals, precious metals, or Earth-abundant metals) and the oxidant. We have found it more useful to classify them according to the oxidant used, as metal-based oxidants and metal-free oxidants seem to favor different mechanistic variations. All steps in the full catalytic cycle are analyzed, and issues concerning selectivity and influence of the oxidant are considered.

KEYWORDS: oxidative coupling, DFT calculations, mechanisms, oxidant, single electron transfer, homogeneous catalysis



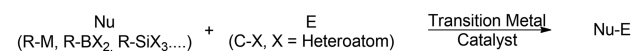
1. INTRODUCTION

The selective formation of bonds between carbon and other carbon or heteroatom centers is one of the main challenges of synthetic chemistry. In the last decades of the past century, cross-coupling reactions based on transition-metal catalysis emerged as a powerful tool to build molecular complexity.¹ Work in the topic was indeed recognized by the Nobel Prize in 2010, which was awarded to Heck, Suzuki, and Negishi.² This methodology is based on the coupling of two different reactants, one with a more electrophilic carbon center (bound to halide, triflate, ...) and another with a more nucleophilic one (bound to a more electropositive atom). The coupling of nucleophilic and electrophilic centers has the advantage of an electroneutral process, as the formal charges on the remaining fragments are neutralized. However, it has two limitations. The main one is the usual need of prefunctionalization of the substrate. A second problem derives from that fact that the electropositive atoms bound to the nucleophilic carbon, such as boron, silicon, tin, or zinc, are usually relatively uncommon in organic chemistry (Scheme 1, top equation). These atoms go usually to subproducts, which are not easy to separate. In this aspect, the poor atom economy of classical cross-coupling is not an ideal fit with the “green chemistry” concept, which tries to minimize the human impact on the environment, making processes more sustainable.³

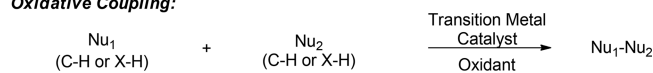
Oxidative coupling is an emerging alternative to cross-coupling, which can deal with some of the problems mentioned above.⁴ In oxidative coupling, two nucleophilic centers, that can be carbon, oxygen, nitrogen, or others, are coupled (Scheme 1, middle equation). The basic concept is similar to cross-coupling, but there are significant practical differences. The nucleophilic centers are often bound to hydrogen, which does

Scheme 1. Cross-Coupling versus Oxidative and Reductive Couplings

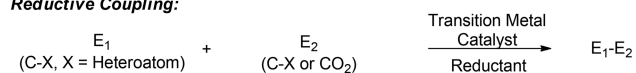
Classic Cross-Coupling:



Oxidative Coupling:



Reductive Coupling:



not require prefunctionalization, and there is a need for an external (or internal) oxidant to keep the entire process electroneutral.

The lack of prefunctionalization is mostly an advantage, although it may limit group tolerance and create the need of directing groups to achieve good selectivities in the case of competing C–H bonds for activation. The need for an external oxidant is mostly a disadvantage, as the byproducts of their reduction have to be eliminated, except in the case where dioxygen can be applied, producing only water as waste. Oxidative coupling is thus a related and complementary approach to cross-coupling, which may be able to replace it since it is more efficient in many cases. Although it will not be discussed here, we must mention that the reverse methodology, namely reductive coupling, is also being developed, especially to

Received: August 31, 2017

Revised: December 22, 2017

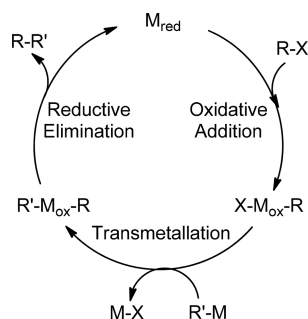
Published: December 22, 2017

introduce CO₂ as an electrophile (Scheme 1, bottom equation).⁵

We are aware that other redox processes are becoming key reactions in modern chemistry. Some of them could be included in a more general definition of oxidative coupling but have not been considered for this perspective. For example, photoredox catalysis often leads to chemical couplings such as C–C or C–N bond formations,^{6,7} but the main mechanistic feature of this methodology is the interaction of light with the substrate or the catalyst.⁸ Something similar occurs for electrochemical oxidations,⁹ that usually involve a formal oxidative coupling but have a mechanism based on electrode electron transfers,¹⁰ or stoichiometric oxidations, such as those in iodine(III)-mediated chemistry.¹¹ Although certainly relevant, the mechanisms of these transformations have different features from those discussed in this work.

The mechanistic picture for cross-coupling is quite clear nowadays, and it is a good starting point to discuss that of oxidative coupling. The cross-coupling catalytic cycle consists of three main steps: oxidative addition, transmetalation, and reductive elimination (Scheme 2). Other minor steps such as

Scheme 2. Schematic Catalytic Cycle of the Cross-Coupling Reaction



the aggregation of intermediates, isomerization, or activation of the reactant with a base can also be present in the catalytic cycle. In the most common examples, a C–halogen bond is activated through oxidative addition, formally oxidizing the metal by two units. Then, an electronegative carbon replaces the halogen in the metal coordination sphere by transmetalation. Depending on the counterpart of the electronegative carbon reactant, which is usually based on non-abundant elements in organic compounds such as B, Si, and Zn, different cross-coupling protocols have been reported, covering a wide range of chemical transformations. Finally, the oxidized metal undergoes a reductive elimination step, releasing the product and regenerating the catalyst. This cross-coupling mechanism has been extensively studied by computational chemistry, mainly by density functional theory (DFT) methodology,^{12–15} and this has contributed substantially to the characterization of this mechanism.

The problem in the translation of mechanistic concepts from cross-coupling to oxidative coupling is in the role of the oxidant, which must take two (or more) electrons from the reactants to keep the entire process electroneutral. This seemingly small change critically affects the reaction mechanism; in fact, in many cases, it is not clear how and when the oxidant participates in the catalytic cycle. The seminal work by Miura and Satoh on the oxidative coupling of alkynes and benzoic acid presents a clear example of these questions.^{16,17} It was found that, depending on the metal (Rh/Ir) and depending

on the oxidant (silver or copper acetate), the chemoselectivity of the reaction is reversed, proving an active role of the oxidant during the reaction. Thus, some important questions have risen from an experimental point of view, such as

- (1) What is the specific role of the oxidant in the reaction?
- (2) Why do specific “magic” combinations of oxidant/additives are especially efficient?
- (3) What is the actual active catalyst in solution?

In this perspective, we intend to summarize the mechanistic knowledge that has been collected on oxidative coupling in recent years, with a focus on the contribution from calculations. We will first discuss briefly C–H activation, which is common with other processes such as direct arylation, and has been discussed previously. We then will focus on the more specific aspects of oxidative coupling. We have classified the results as a function of the nature of the oxidant, because we consider this to be mechanistically significant.

2. COMPUTATIONAL METHODS

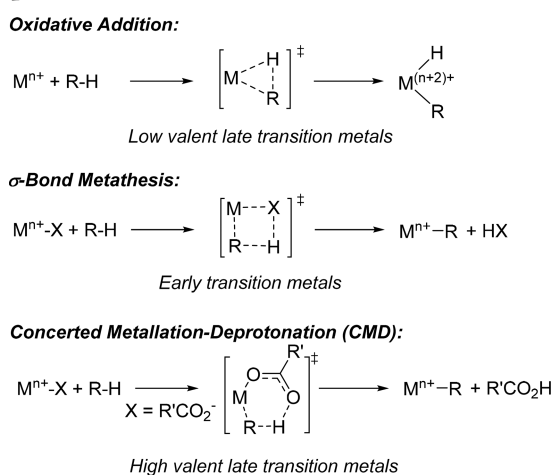
In this perspective, we focus on the recent progress in the computational characterization of oxidative coupling mechanisms. In this section, we report a brief summary of the most common methodologies that are being employed in this area. Density functional theory (DFT) is clearly the preferred method for the computational study of these reactions. DFT has been extensively used in many different chemical processes, and, in organometallic chemistry and homogeneous catalysis, it is clearly the current method of choice.¹⁸ Regarding the specific functionals employed, both (meta)GGA and hybrid functionals are used, most often B3LYP,^{19,20} M06-L,²¹ M06,²² and B97D.²³ The amount of HF exchange in the functional is important when open-shell species participate in the reaction pathways, and consequently, benchmarking of the selected method, either vs experiment or vs highly accurate calculations, is extremely important on the field. The contribution of dispersion corrections is also nowadays widely recognized, and is often introduced as an explicit term (D2²³ or D3²⁴) or indirectly through heavily parametrized functionals such as those in the M06 family. Implicit solvent models (such as SMD)²⁵ in optimizations to simulate the reaction medium are also now the common practice.

3. THE MECHANISM OF C–H (OR X–H) ACTIVATION

Oxidative coupling often involves the direct activation of two C–H or X–H (where X is a heteroatom) bonds, without prefunctionalization. This step is not exclusive of oxidative coupling. The mechanisms of C–H activation have indeed been actively explored both experimentally^{26–29} and theoretically^{30–33} during the last decades.

The most common reaction pathways are summarized in Scheme 3. The specific mechanism of C–H activation is dependent on the metal and the organic fragment. If a metal can easily reach a higher oxidation state, the oxidative addition of the C–H bond would be the most preferred mechanism. This is usually the case in low-valency late transition metals, which can increase the oxidation state of the metal by two units.³⁴ σ -Bond metathesis consists of the addition of the C–H bond to an activated M–C or M–H bond, typically on early transition metals. Finally, the most widely explored C–H activation mechanism, and the one that usually occurs in oxidative couplings, is the concerted metalation–deprotonation (CMD).^{35–37} In this case, an external base, most often a

Scheme 3. C–H Activation Mechanisms by Transition-Metal Complexes



carboxylate attached to the metal, helps in the deprotonation of the activated C–H bond. Macgregor recently reported a comprehensive review on the field that collects the large number of systems in which CMD is the C–H activation mechanism.³⁸

4. CLASSIFICATION OF OXIDATIVE COUPLING REACTIONS

Several metals have been shown to catalyze oxidative couplings, those more common being rhodium,^{39–42} palladium,^{43,44} and ruthenium.^{45,46} Recently, other non-noble metal centers, such as cobalt⁴⁷ or copper,⁴⁸ have also been developed as less-expensive and less-toxic alternatives, although the efficiency of these systems is still far from those based on precious metals. However, a classification of reactions based on catalysts does not seem appropriate, because similar catalysts seem to produce diverse mechanisms.

The nature of the external oxidant seems to be a more critical factor on the mechanism. Thus, we decided to classify the oxidative coupling reactions discussed in this perspective according to the type of oxidant used. We distinguish two different main types, the metal-based oxidants and the metal-free oxidants (Scheme 4).

5. METAL-BASED OXIDANTS

Traditionally, metal-based oxidants have been the most used to perform oxidative coupling reactions. The appropriate reduction potential, as well as the basic character of the carboxylate ligands usually attached to the oxidant, makes these transition-

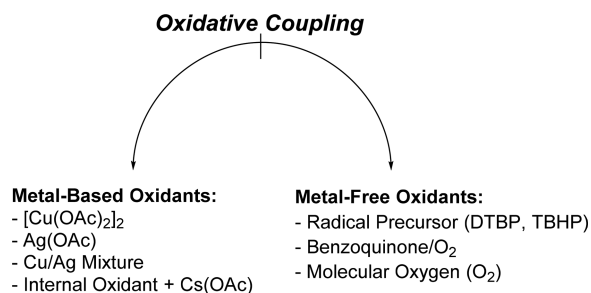
metal salts the option of choice to assist both in the activation of C–H bonds and regeneration of the catalyst. The most common oxidants of this type is probably copper(II) acetate, which has been used extensively for years, especially in rhodium and ruthenium catalysis, as privileged oxidant.^{49–53} The other common salt that is used as an oxidant is the silver(I) acetate.^{54–57} This oxidant can also efficiently trap the Cl atoms of the metal catalyst used (normally $[\text{Cp}^*\text{RhCl}_2]_2$ or $[(p\text{-cymene})\text{RuCl}_2]_2$). For this reason, sometimes both metal salts are combined, with copper(II) acetate as the main oxidant and silver(I) acetate as a chloride abstractor.^{58,59} In this section, we have also included the internal oxidants. Formally, there is no metal-based oxidant in these reactions, because the internal oxidant is an electron-poor bond, normally a N–O bond, that traps two electrons in the process and then acts as the oxidant. However, the conditions used in these reactions, and the combination with some acetate salt (commonly CsOAc) are very similar to those used on Cu- or Ag-assisted reactions. Herein, we report some specific mechanistic examples where DFT calculations have been demonstrated to be a valuable tool to understand the reaction features.

5.1. $[\text{Cu}(\text{OAc})_2]_2$. Copper(II) acetate has been the most used oxidant in this type of reaction. It has demonstrated very interesting properties, in terms of efficiency, reaction selectivity, and reaction scope, especially in combination with Rh and Ru species as main catalysts. Specific roles of this oxidant in the catalytic cycle have been proposed by some authors, but its full understanding is still a matter of study.

The first examples of DFT calculations focused mainly in the C–H activation step, normally through the concerted metalation–deprotonation (CMD) transition state assisted by the acetates in the reaction medium. For example, Hu, You, and co-workers reported the mechanism for the C–H activation of imidazole and thiophene.⁶⁰ In this work, $\text{Pd}(\text{OAc})_2$ activates efficiently both C–H bonds, first that in imidazole and later that in thiophene, to promote the cross-oxidative coupling of these two heteroarenes. However, the reaction barrier reported for the C–H activation of thiophene (~ 40 kcal/mol) was very high, probably because of the absence of dispersion in the calculations. These energies are unrealistic, confirming the importance of the choice of the method.

Davies, Macgregor, and co-workers further highlighted the importance of dispersion effects in DFT calculations of C–H activation processes.⁶¹ They successfully studied the full catalytic cycle of the oxidative coupling of pyrazoles with alkynes catalyzed by rhodium or ruthenium species. Kinetic isotope effect (KIE) experiments had shown that the KIE was primary for Rh catalyst and almost negligible for Ru complex. DFT calculations showed that the highest barrier for the catalytic cycle in the Rh system was the CMD process on the pyrazole ring, whereas in the case of Ru, the CMD of the C–H activation step is barrierless on the free-energy surface, the $\kappa^2\text{-}\kappa^1$ isomerization of the acetate being the highest barrier in the C–H activation process. This conformational change previous to the C–H activation process has a barrier higher by 2.8 kcal/mol. For both metals, the formation of diacetate monomer derivative $(\text{CpRh}(\text{OAc})_2)$ or $(p\text{-cymeneRu}(\text{OAc})_2)$ from the initial chloride dimer precursors was assumed, considering the copper acetate both as an oxidant and as an acetate donor. The following steps, alkyne insertion and reductive elimination were lower or very similar in energy to the C–H activation. The regeneration of the initial catalyst was not studied in this case, although the reaction works

Scheme 4. Classification of Oxidative Coupling Reaction Based on the Nature of the Oxidant



stoichiometrically in the absence of oxidant when a good acetate source (NaOAc) is used.

Recently, the same authors expanded the initial study with a comprehensive paper on the Rh(III)-catalyzed oxidative coupling of nitrogen-derived heterocycles with alkynes.⁶² The solvent dependence of the C–H activation process was successfully explained. They found two different mechanisms for this step: the classic intramolecular CMD process and the nondirected intermolecular C–H activation. The relative barriers of both processes, with respect to the solvent, were explained by the charge of the system in both transition states. In the case of the CMD process, one acetate ligand is replaced by the substrate, resulting in a charged species, favored in polar solvents. The intermolecular process remains neutral during the reaction pathways and is therefore favored in nonpolar solvents. They extended those results to the reductive elimination step, where the cationic or neutral character of the 7-member metallacycles is key for the activation barriers (Figure 1). C–C

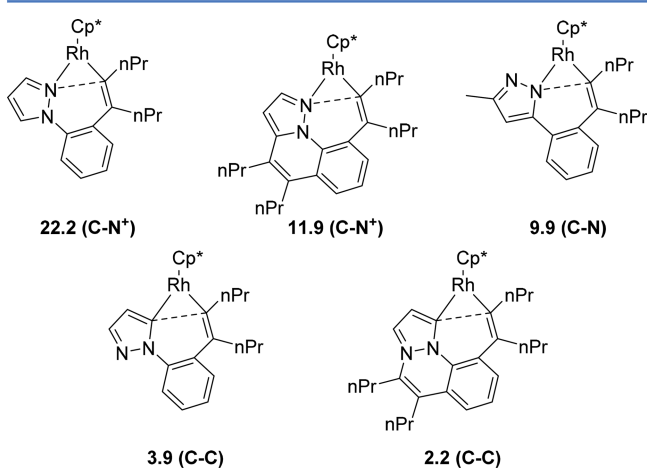


Figure 1. Reductive elimination step on several C–N and C–C coupling in 7-member rhodacycle intermediates. Values shown represent free-energy barriers (in kcal/mol).

bond formations are extremely fast, with barriers below 4 kcal/mol, independent of the charge of the system. However, C–N bond formation are strongly affected by the charge going from 22.2 kcal/mol barrier for C–N⁺ to just 9.9 kcal/mol in neutral C–N bond.

An asymmetric version of an oxidative coupling reaction was analyzed by DFT methods by Zheng, You, and co-workers.⁶³ A chiral Cp ligand on a Rh(I) precatalyst, that is activated by (BzO)₂, was used to promote the catalytic dearomatization of 2-naphthols. Again, copper acetate was only considered as a final oxidant and as an acetate donor. The mechanism consisted of a C–H activation directed by the hydroxo group in the reactant, followed by alkyne insertion, keto/enol tautomerization, and a reductive elimination that yields the product enantioselectively. The oxidant was calculated as a dimer, providing a very exergonic reaction. It is noteworthy to highlight here the importance of metal salts speciation in organic solvents. The authors found that the first C–C bond formation step (the alkyne insertion) was the enantioselectivity-determining step, because of the irreversible barrier and the impossible epimerization of intermediates after this step. The calculations predicted a difference between both transition states (the *pro-S* and *pro-R*) of 2.9 kcal/mol, in close agreement with the experimental ratio (97:3) to the (*S*) enantiomer.

Mascareñas, Gulías, and co-workers analyzed an intramolecular version of a Rh(III)-catalyzed oxidative annulation both experimentally and theoretically.⁶⁴ The reaction consists of five different steps: the N–H activation, the C–H activation, the migratory insertion of the alkyne, the reductive elimination, and the regeneration of the catalyst. Again, Cp^{*}Rh(OAc)₂ was considered to be the active species, and the most remarkable point was that the alkyne insertion occurs into the Rh–N bond instead into the more common Rh–C bond, because its energy barrier is 2.8 kcal/mol lower. This feature is related to the intramolecular character of the reaction.

Interestingly, all the cases discussed above considered the oxidant as a simple regenerator of the catalyst. As far as we know, only two examples have considered explicitly the role of copper(II) acetate during the reaction pathway. The hypothesis of a more elaborate role for copper(II) acetate is moreover favored by the kinetic experiments carried out by Jones and co-workers, who observed, using ultraviolet–visible light (UV-vis) techniques that, in mixtures of [Cp^{*}Rh₂Cl]₂, [Cu(OAc)₂]₂ and a strong acetate donor such as NaOAc, only one chloride is easily substituted to form the [CpRhCl(OAc)] in solution.⁶⁵ Morokuma and co-workers introduced the issue of a possible active role for Cu(OAc)₂ in a DFT mechanistic study on the Rh(III)-catalyzed C–H activation of 8-methylquinoline.⁶⁶ They suggested that there was no free acetate in the medium and Cu(OAc)₂ solvated with DMF molecules acted as a base in the reaction, efficiently activating the sp³ bond. The results of this paper have been questioned in the recent review of Macgregor and co-workers, because of the lack of diffuse functions and the difficult rationalization of the H/D exchange experiments, which shows this step to be reversible.³⁸ This highlights the difficulties in describing the speciation of this metal salt in organic coordinated solvents such as DMF, as has been demonstrated by experiments.⁶⁷ This particular reaction finishes with a hydrogen migration and therefore, it is not an oxidative coupling, so copper diacetate should have a role in the catalytic cycle apart from the classical role as oxidant.

In this concern, our group carried out the mechanistic study of the rhodium-catalyzed oxidative coupling between benzoic acid and alkyne.⁶⁸ Interestingly, the chemoselectivity of this reaction was dependent on the oxidant, yielding very good selectivity to the isocoumarin product only when copper(II) acetate was used. The key feature of this reaction is the competition between the reductive elimination and the CO₂ extrusion process, and if CpRh(OAc)₂ was considered as the catalyst, the predicted selectivity was wrong (Figure 2). We found a lower energy pathway in which copper acetate is associated throughout the catalytic cycle with the rhodium catalyst, resulting in a cooperative reductive elimination step which explains the selectivity successfully. Remarkably, the two electrons that are released from the organic moiety during the C–O bond formation go to the different metals: one to the rhodium center, generating Rh(II) and the other to the copper dimer, reducing it by one electron. This is a clear example in which the catalytic cycle operates through active participation of the oxidant.

5.2. AgOAc. Silver salts, mainly AgOAc (but also Ag₂O or Ag₂CO₃), are also a good option as oxidant, either as a final oxidant or as a catalytic agent. Moreover, Ag cations can efficiently trap the Cl atoms from the catalyst precursor, generating the active species with carboxylates attached to the main metal center. Several studies analyzed this type of reaction

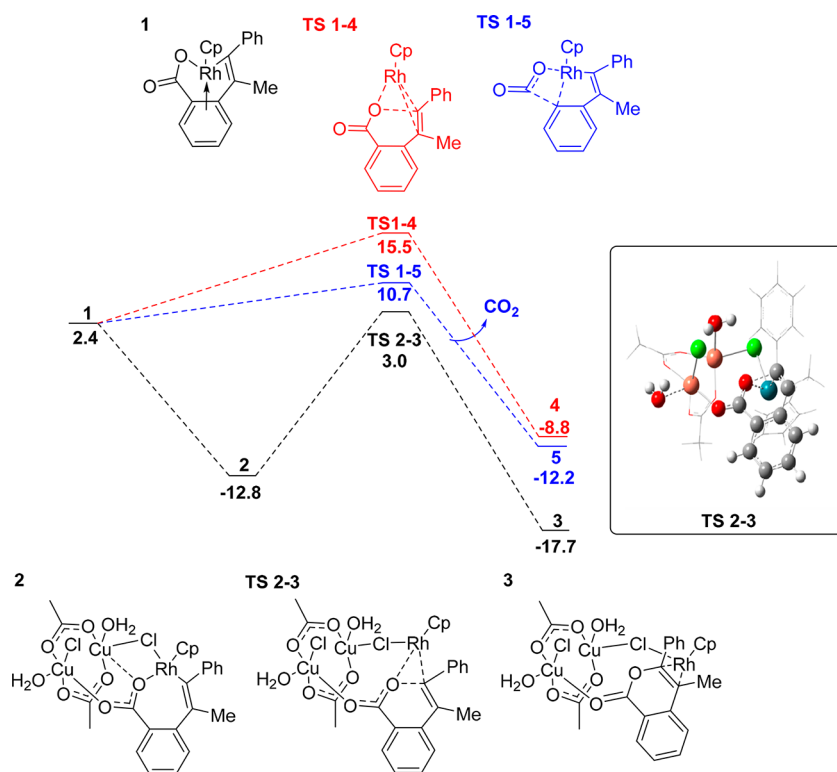


Figure 2. Free-energy profile of the chemoselective step in the oxidative coupling of benzoic acid and alkyne catalyzed by Rh(III) with the cooperative effect of copper(II) acetate. Values shown are energies (in kcal/mol), in reference to the separated reactants.

computationally but without focusing on the role of silver salt.^{69,70}

Houk and co-workers analyzed the factors that affect the selectivity in the *meta*-C–H activation of arenes, using a nitrile-containing template to enhance the reactivity at this position.⁷¹ Apart from the role as oxidant, they found a heterobimetallic mechanism based on PdAg(OAc)₃ dimeric structure, in which the size of the cluster is appropriate for activating selectively the *meta* position of the arene (Figure 3). The nitrile used in the

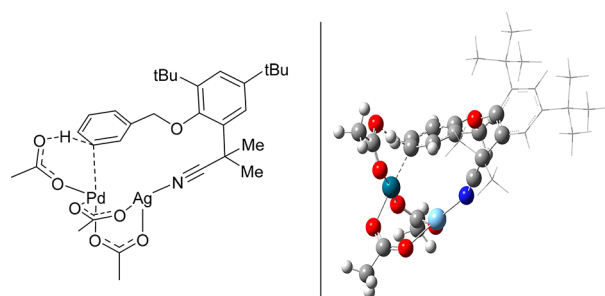


Figure 3. Transition state of the CMD of the *meta* position of an arene, using a nitrile template and a heterometallic dimer based on Pd/Ag interaction.

template coordinates with the Ag cation, generating a good geometry for the CMD of the *meta*-C–H bond by the Pd center, which is the rate- and selectivity-determining step. Thus, it is another example of the active role of the oxidant in the catalytic cycle.

Another example of the DFT characterization of the role of silver salts was carried out by Ison and co-workers.⁷² They analyzed the oxidative coupling of benzoic acid and alkynes catalyzed by [Cp*IrCl₂]₂ complex using AgOAc as oxidant in

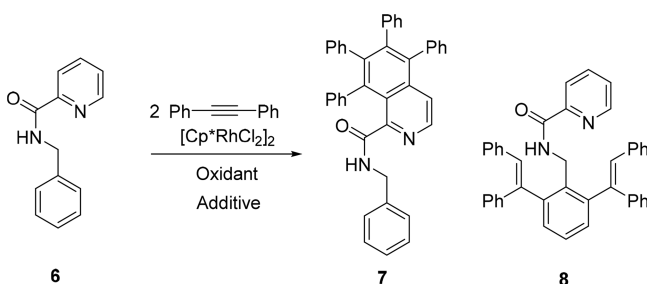
dimethylsulfoxide (DMSO) to form isocoumarins. Experimentally, they demonstrated the formation of the Cp*Ir(OAc)₂ as active species, which can activate the *ortho*-C–H bond of benzoic acid stoichiometrically. In addition, they suggested that the rate-determining step was the alkyne insertion. This was further proved by DFT calculations, although dispersion interactions were not considered and the results can be misleading. Interestingly, they calculated the regeneration of the catalyst by silver acetate. Once O–H and C–H were activated and the alkyne was inserted, they analyzed the reductive elimination pathway from Ir(III) and they also explored the possibility of forming previously Ir(IV) or Ir(V) with the oxidant. The last options were discarded due to the high energy. Finally, when Ir(I) and the isocoumarin product were produced, the regeneration of the initial catalyst occurred via two consecutive single electron transfer (SET) steps from Ir center to AgOAc. The product is released after the first SET, at the Ir(II) center, and then the second SET is exergonic, to regenerate Ir(III) species.

5.3. Cu/Ag Mixture. Several experimental reactions use a combination of copper(II) acetate as the oxidant (1–2 equiv) and catalytic amounts of a silver salt in combination with Rh or Ru precursors. This combination takes the advantages of both salts. On one hand, copper acts as the most efficient oxidant for oxidative coupling reactions, and, on the other hand, silver activates the main catalyst precursor, removing the Cl atoms and forming the acetate-derived active species. Lan, Huang, and co-workers analyzed the influence of each species separately under the same experimental conditions (140 °C and 16 h in toluene as solvent) and they found an improvement of the yield from 25%, when only copper(II) acetate was used, to 65% when silver and a base were added to the reaction medium.⁷³ However, they did not consider these effects in the DFT

calculations, calculating the catalytic cycle with $\text{CpRh}(\text{OAc})_2$ as the active catalyst. The same happens in the ruthenium-catalyzed oxidative coupling of arenes and alkenes reported recently.⁷⁴

Probably, the best example of the Cu/Ag cooperation is the divergent aryl/heteroaryl functionalization of picolinamides with alkynes, depending on the oxidation state of the main catalyst, Rh(I) vs Rh(III).⁵⁹ Carretero and co-workers explored the influence of the oxidant/additive combination in this reaction. Surprisingly, only when copper and silver were mixed, the reaction selectively yields the oxidative coupling product (Table 1). However, if copper acetate is used, the reaction gives

Table 1. Oxidant/Additive Influence in the Reaction of Picolinamide with 1,2-Diphenylalkyne Reported by Carretero and Co-workers⁵⁹



oxidant	additive	conversion (%)	7/8 ratio (%)
$\text{Cu}(\text{OAc})_2$		47	21/79
	$\text{AgSbF}_6/\text{NaOAc}$	46	<2/>98
$\text{Cu}(\text{OAc})_2$	AgSbF_6	>98	>98/<2

mixtures and if silver acetate (produced from a silver salt and sodium acetate) is used, the reaction gives the Heck alkenylation product selectively.

DFT calculations demonstrated that two catalytic cycles can operate in the same substrate, one from Rh(III) and the other from Rh(I). The relative influence of both pathways is

extremely correlated with the oxidant/additive combination used (Figure 4)

5.4. Internal Oxidant + Cs(OAc). The last group of reactions in this section consists of the processes with an internal oxidant, usually an electron-poor N–O bond. This oxidant has formally no metal, but the reaction substrates as well as the main catalysts used are very similar to those discussed above. In addition, these metal catalysts are usually combined with good acetate donors, to generate active species such as $\text{Cp}^*\text{Rh}(\text{OAc})_2$ or related complexes.^{75,76}

The difference, with respect to the other oxidants, is that the initial catalyst is regenerated by oxidative addition to this electron-poor N–O bond. Two different cases have been described: the oxidation of the bond before and after reductive elimination. The first one generates the metal in a very high oxidation state, as Rh(V), and this facilitates the next reductive elimination. The other possibility implies the formation of Rh(I) and the regeneration of Rh(III) by oxidative addition.⁷⁷

Those different mechanisms allow one to control the chemoselectivity of the reaction, especially playing with the nature of the O group on the N–O bond. Xia and co-workers studied this effect in the oxidative coupling of benzamide derivatives (A) with olefins computationally.⁷⁸ They demonstrated that the nature of the R group in the N-OR moiety determines the formation of the aryl olefination product (F) or the cyclic amide formation (I), as is shown in Figure 5. The reaction starts for both substrates (OR groups = OMe or OPiv) following the same steps: N–H activation and C–H activation via CMD transition state (B), and olefin insertion to form the 7-membered rhodacycle intermediate (C). However, the stability of this intermediate is tremendously influenced by this OR group. When OMe is used, the rhodacycle is not stable and the arene olefination occurs through a β -hydrogen elimination, forming D, followed by N–H reductive elimination, generating Rh(I) intermediate E. The catalyst is regenerated by MeOH elimination assisted by HOAc. In contrast, when OPiv is used as an internal oxidant, the 7-membered rhodacycle intermediate is stabilized by the OPiv

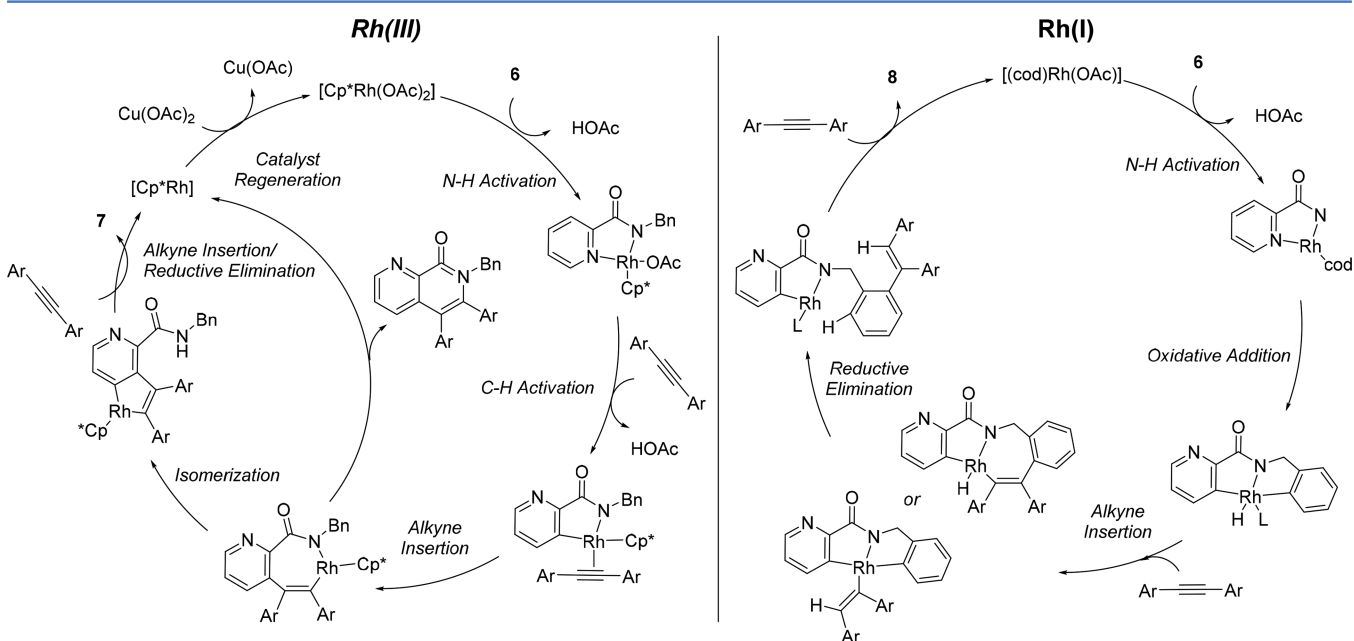


Figure 4. Proposed competing catalytic cycles of Rh(III) vs Rh(I) mechanisms on the reactivity of picolinamides and alkynes.

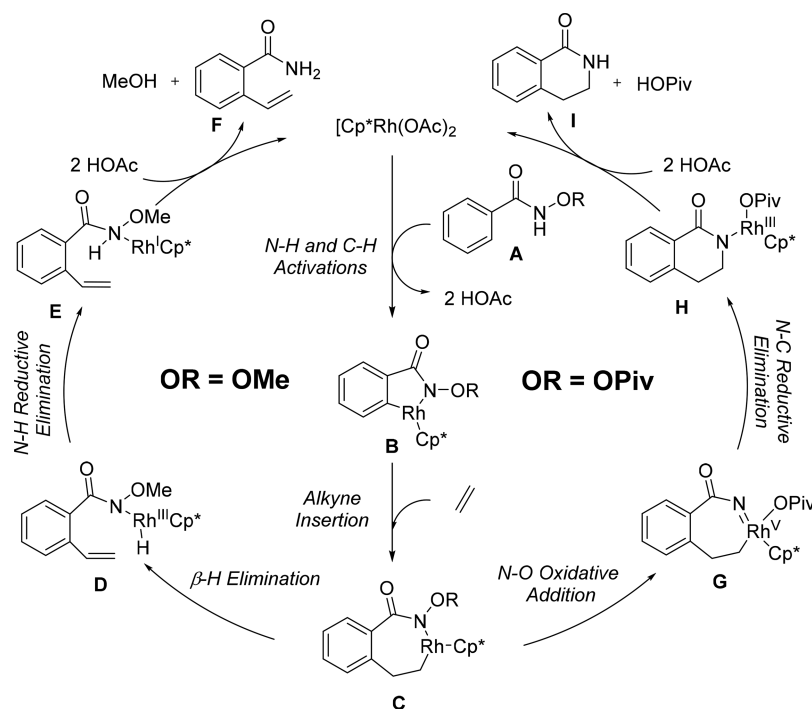


Figure 5. Catalytic cycles of the internal oxidant-controlled mechanism of oxidative coupling of benzamide derivatives and ethylene.

group via acyloxy carbonyl coordination. Then, N–O bond is broken, forming Rh(V)-nitrene intermediate **G** that undergoes easily the reductive elimination to form the cycle amide intermediate **H**, that release the product **I** after nitrogen protonation by HOAc.

Another interesting issue of this reaction is the effect of the additives. Sunoj, Schaefer, and co-workers analyzed by means of DFT the influence of silver acetate and cesium fluoride in the palladium-catalyzed *ortho*-amination of *N*-arylbenzamide.⁷⁹ Experimentally, the yields increase considerably when both additives are used, using the same reaction conditions (130 °C and 18 h). They demonstrated that the C–H activation process is strongly influenced by those additives, lowering the barrier from 28.1 kcal/mol to <10 kcal/mol. The cooperative transition state is shown in **Figure 6**. A more recent study of the authors expanded the cooperative effect of Pd/Ag to the complete catalytic cycle, demonstrating that both metals favor the reaction along all of the elementary steps.⁸⁰

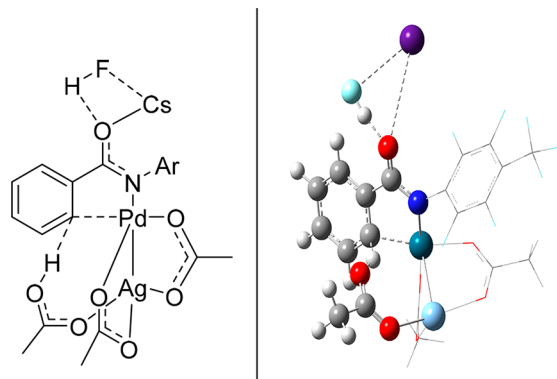


Figure 6. Cooperative C–H activation of an arene by combination of Pd/Ag/Cs in the transition state.

6. METAL-FREE OXIDANTS

The second group of oxidants is based on metal-free compounds such as organic molecules or molecular dioxygen. These have the advantage of yielding less-toxic subproducts, increasing the sustainability of the oxidative coupling processes. However, the reactions seem less efficient and further optimization will be necessary. We consider three different cases: organic compounds that act as radical precursors, benzoquinone/O₂ and molecular dioxygen. Radical precursors, such as di-*tert*-butyl peroxide (DTBP) or *tert*-butyl hydroperoxide (TBHP), are usually combined with first-row transition metals as the main catalyst, as these catalysts are the most appropriated for one-electron oxidations, and therefore, to react with radicals.⁸¹ The second type discussed here is the molecular-dioxygen-based oxidative couplings.^{82–84} This oxidant is very appealing, as it produces only water as byproduct and is very inexpensive. However, the activation of the triplet ground state of the O₂ molecule is challenging. We have selected some specific examples that use DFT calculations to rationalize the reaction mechanism.

6.1. Radical Precursors. The ability of organic peroxides to promote radical formation has been used to perform oxidative coupling reactions. Normally, a transition-metal catalyst is needed to increase the selectivity and the efficiency of the reaction. Lei and co-workers reported a C–N bond formation through a radical oxidative cross-coupling catalyzed by copper complexes using DTBP as an oxidant.⁸⁵ They demonstrated that Cu(II) can coordinate *N*-methoxybenzamide and under radical conditions, the N–H bond is broken homolytically to form a nitrogen-centered radical. The resulting intermediate, characterized by DFT calculations as a triplet diradical, is persistent and can be trapped by 5,5-dimethyl-1-pyrroline-*N*-oxide (DMPO). Interestingly, B3LYP calculations showed that this triplet state was more stable than the corresponding Cu(III) compound, by 25.7 kcal/mol. These DFT results were the starting point for the evaluation of the cross-coupling of this

activated nitrogen with carbon compounds. It was found that the allylic position of cyclohexene was the most appropriate to form the C–N bond, with yields up to 83% and a wide scope. The same strategy was explored to promote the oxidative coupling of this amide with tetrahydrofuran (THF) under Cu or Ni catalysts.⁸⁶

Fu, Yu, and co-workers analyzed computationally the oxidative coupling of benzamide and toluene catalyzed by a Ni(II) complex.⁸⁷ They showed that this type of reaction is extremely complicated, from a mechanistic point of view, because different pathways are plausible. First, the N–H and C–H bond of the benzamide are activated by the PPh₃Ni(II) complex. From this point, three different pathways were calculated (Figure 7). The first one is based on the reaction of

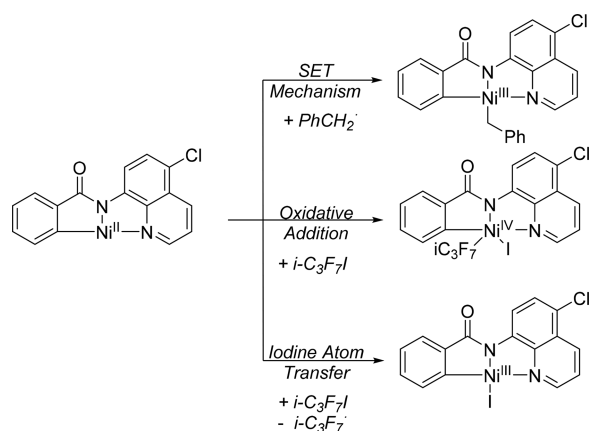


Figure 7. Divergent pathways from Ni(II) intermediate in the oxidative coupling of benzamide and toluene.

the Ni(II) intermediate with the benzyl radical generated by single electron transfer from an perfluoroalkyl iodide (*i*-C₃F₇I) compound. The direct generation of this radical was thermodynamically too high for a thermal process (36.1 kcal/mol). The second option consisted of the oxidative addition of *i*-C₃F₇I to the Ni(II) intermediate, but the energy of this step was estimated to be >45 kcal/mol (the transition state could not even be located). Finally, the productive pathway was the iodine-atom transfer mechanism with an overall barrier of 30.0 kcal/mol. This mechanism demonstrated the importance of single electron transfer steps in radical oxidative coupling and the effect of Ni(II) as an electron donor in the process.

A last example selected for radical oxidative coupling was reported by Fang and co-workers, and it consists of a C–O coupling catalyzed by Cu species.⁸⁸ This reaction is strongly dependent on the oxidant and DFT calculations provided a successful explanation on the oxidant effect (Figure 8). Small peroxides, such as TBHP promotes the radical pathway through a single electron transfer from Cu(I) to Cu(II). Then, Cu(II) reacts with the dimethyl formamide (DMF) radical generated in the reaction medium to form the Cu(III) intermediate. In contrast, *meta*-chloroperoxybenzoic acid (mCPBA) prefers the oxidative addition pathway to form directly a Cu(III) species. After that, the chlorobenzoate can deprotonate the ethyl acetoacetate intermolecularly. Finally, the hydroxo group activates the C–H bond in DMF and the product is formed via reductive elimination. Sterically hindered oxidants, such as DTBP or dibenzoate peroxide (BP), are not productive, because the oxidative addition prevents the DMF coordination, inhibiting the C–H activation.

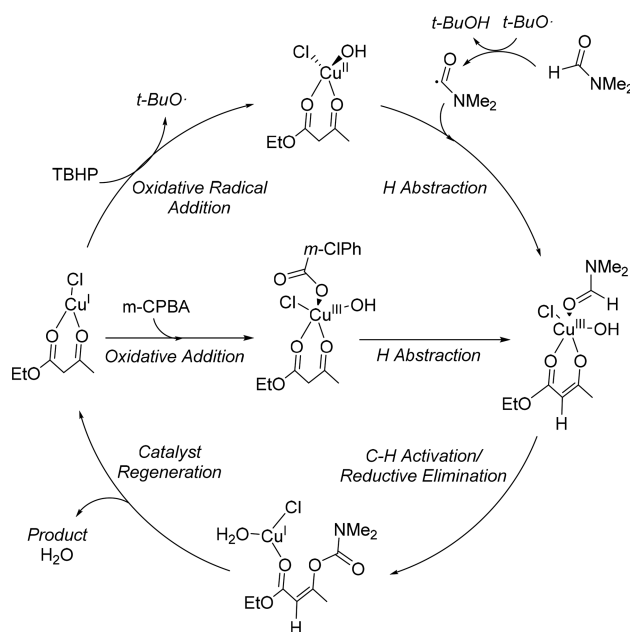


Figure 8. Oxidant effect in the mechanism of the oxidative coupling of ethyl acetoacetate and dimethylformamide (DMF).

Interestingly, most of the radical oxidative couplings can be described with a catalytic cycle starting with catalyst oxidation. The organic oxidant first activates the substrate or the catalyst, and the reaction occurs exothermically until the regeneration of the initial species.

6.2. Benzoquinone/O₂. The use of benzoquinone and its derivatives as oxidants for oxidative couplings is appealing, especially in Pd catalysis, because of the ability of this organic oxidant in the stabilization of Pd(0) intermediates, thus hindering catalyst decomposition. Benzoquinone can be used stoichiometrically to regenerate the catalyst,⁸⁹ or in catalytic amounts using molecular oxygen as the final oxidant.⁹⁰

Liu and co-workers recently reported two interesting examples in this concern. The first one is based on the oxidative carbocyclization and arylation by Pd catalysts, analyzing the specific role of the solvent in the chemoselectivity.⁹¹ The other example studied in detail the competitive pathways for the carbocyclization and alkoxycarbonylation of bis-allenes.⁹² However, the specific role of benzoquinone was not explored in any of these studies.

From a mechanistic perspective, Schoenebeck, Sanford, and co-workers demonstrated the importance of benzoquinone to promote the reductive elimination step in the oxidative C–H functionalization of arenes and benzoquinolines.⁹³ They found that the barrier for C–C bond formation is reduced when benzoquinone is coordinated to Pd by 20–30 kcal/mol, in comparison with the same intermediate with acetate coordinated or with a vacancy (Figure 9). This specific example again highlighted the relevance of including additive or oxidants in the computational study of catalytic cycles.

6.3. Molecular Dioxygen (O₂). As we discussed in the Introduction, one of the main appeals of the oxidative coupling reactions is to reduce the waste product formation in comparison with the classic cross-coupling reactivity. In this sense, molecular dioxygen is an optimal oxidant. It is very inexpensive, clean, and the usual byproduct is simply water. However, the direct use of this oxidant is a challenge for several reasons: O₂ is very stable, both thermodynamically and

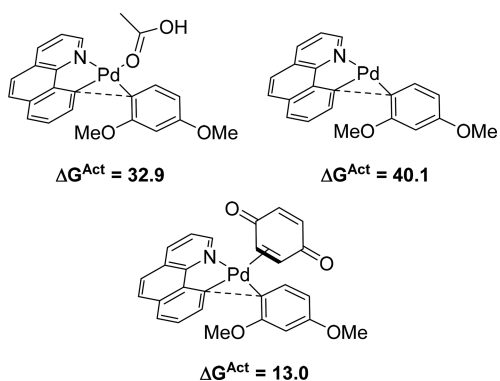


Figure 9. Comparison of transition states for the reductive elimination step in Pd-catalyzed oxidative C–C bond formation with no ligand, HOAc, or BQ ligands.

kinetically, and the ground state is a triplet, hindering the activation on a singlet potential energy surface. In the last years, several examples have been reported and studies of the reaction mechanisms have started.

For example, Pd(II) diacetate can be used in combination with oxygen and pyridine as a ligand to promote oxidative Heck reactions. Zhang and co-workers studied this reaction computationally, via DFT methods.⁹⁴ They focused mainly on the C–H activation process, which is based on a CMD transition state, activating the arene with a barrier of 31.3 kcal/mol (the rate-determining step). The alkene then is inserted into the Pd–C bond, forming the palladacycle intermediate (Figure 10). After

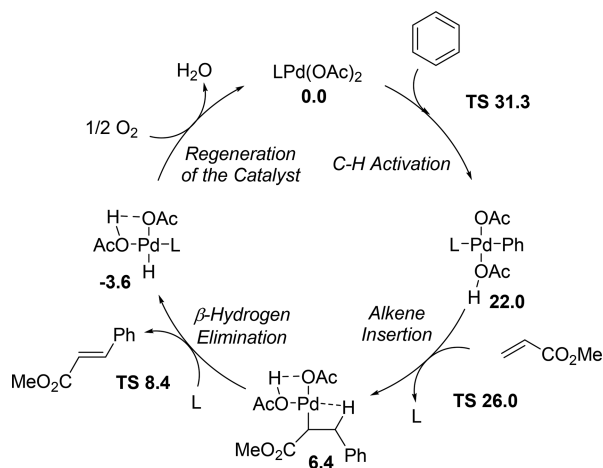


Figure 10. Catalytic cycle of the Heck oxidative coupling of benzene and methyl acrylate catalyzed by Pd(II) with O_2 as an oxidant. Values shown represent free energies (in kcal/mol).

that, there is a β -hydrogen elimination with a small barrier of 1.6 kcal/mol, releasing the product. Finally, Pd(0) is generated, protonating the remaining acetate. This Pd(0) species regenerates the initial catalyst, reacting with molecular oxygen. Only the thermodynamics of this last step was evaluated, with no detailed mechanistic analysis, with overall ΔG° value of -44.7 kcal/mol. In fact, only Pd(II) pathways were analyzed, assuming that the catalytic cycle that operates in the reaction does not depend on the oxidant.

One example that clearly defines the challenges of oxidative coupling reactions with dioxygen is the Glaser–Hay reaction (Figure 11, top).⁹⁵ Although this reaction was reported more

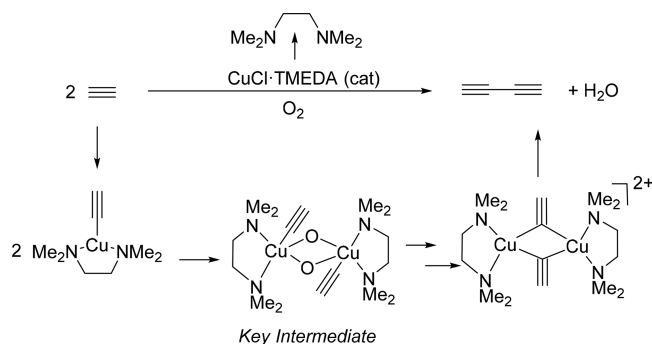


Figure 11. Glaser–Hay reaction of acetylene and the most important steps of the catalytic cycle.

than 100 years ago, the mechanism was not determined in detail until few years ago. Fomina and co-workers reported a preliminary DFT mechanism where the authors suggested that the key step was the dioxygen activation.⁹⁶ This hypothesis was confirmed and expanded in an exhaustive DFT study that was reported by our group.⁹⁷ The reaction is a bimolecular process, where two copper centers activate molecular dioxygen easily forming a Cu(III)–Cu(III) dimer (Figure 11). After protonation of the oxygen bridges, the resulting Cu(III)–OH species reacts with another unit of Cu(I)–acetylide species leading to the Cu(II)–Cu(II) coproportionated product. This species undergoes the reductive elimination to regenerate the catalytic cycle. The nitrogen-based ligand TMEDA acts both as a ligand and as a base during the process, facilitating the deprotonation of the acetylide, which is the rate-determining step of the process, justifying why stronger bases and acidic acetylenes provided higher reaction rates.

The treatment of the triplet state of molecular dioxygen is one of the challenges in these reactions. Huang, Liu, and co-workers tackled this issue in the copper-mediated oxidative coupling of benzothiazole and thiophenol.⁹⁸ The bipyridine–Cu(I) complex first activates the thiophenol group. Then, this group migrates into the electrophilic sp^2 carbon of benzothiazole. The coordination vacancy of Cu(I) is later occupied by the molecular oxygen in the triplet state. Interestingly, oxygen can abstract the hydrogen atom on the Cu–mercaptobenzothiazole in a minimum energy crossing point (MECP) that connects the triplet and the singlet states, going from Cu(II)–O–O \cdot to Cu(I)–OOH and the final product (see Figure 12). In this context, Wang and co-workers have described the mechanism of Pd-catalyzed aerobic C–H functionalization of heterocycles.⁹⁹ In this case, the role of the oxidant has been exhaustively analyzed. The catalyst is a Pd(0) derivative that is initially activated by O_2 . The use of *t*-BuNC as ligand allows this oxidation with a small barrier (8.8 kcal/mol) and a subsequent MECP, from the triplet state to the singlet state, which is even lower in energy. The result of this transformation is the formation of Pd-peroxo cycle singlet intermediate that is able to oxidize the *N*-methoxy amide substrate.

Recently, Liao, Yin, and co-workers studied, both experimentally and theoretically, the Pd-catalyzed oxidative coupling of indole and methyl acrylate, where oxygen is used as a final oxidant.¹⁰⁰ Interestingly, the use of nonredox metal ions, such as Sc or Al, considerably improve the reaction efficiency toward the formation of bid(indolyl)methane derivatives. The proposed mechanism consists in a cooperative Pd/Sc catalytic cycle, where Sc(OTf)₃ assists in the C–H activation of indole

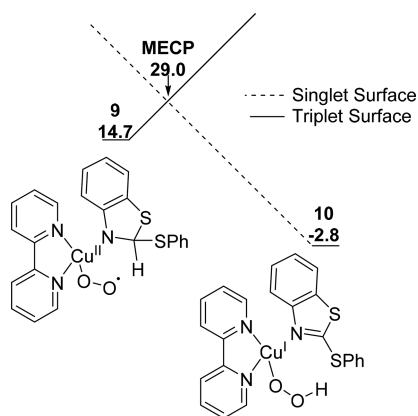


Figure 12. Hydrogen atom abstraction pathway on the oxidative coupling of benzothiazole and thiophenol catalyzed by Cu(I)-bipyridine complex. Energies (in kcal/mol) refer to the reactants.

by CMD mechanism, lowering the barrier from 28.4 kcal/mol to 14.5 kcal/mol. Then, methyl acrylate is inserted and, after a β -hydrogen elimination, the Pd(II)–H intermediates undergo the reductive elimination with an attached acetate. Finally, Pd(0) is reoxidized by molecular oxygen, releasing hydrogen peroxide (detected experimentally) and regenerating the initial Pd(II) catalyst.

The future of these reactions with dioxygen is promising. Recently, Macgregor, Ackermann, and co-workers combined molecular oxygen as oxidant with a first-row transition metal complex as the main catalyst, $\text{Co}(\text{OAc})_2$.¹⁰¹ The reaction consists of the annulation of a benzamide and an alkyne, releasing water as a waste product. Interestingly, the authors suggest that cobalt(II) species is oxidized prior to the reductive elimination step. This is consistent with an active role of the oxidant in the reaction. We are convinced that the flexibility of spin and oxidation states of first-row transition metals will lead to the discovery of new catalytic systems involving dioxygen in the near future.

7. OVERALL PICTURE

The catalytic cycle is complicated. The oxidant, in most cases, seems to play a central role in the mechanism and cannot be confined to a single additional step in an otherwise conventional cross-coupling mechanism. The case for this hypothesis is weaker in the case of metal-based oxidants, such as copper(II) acetate, because of the relative scarceness of

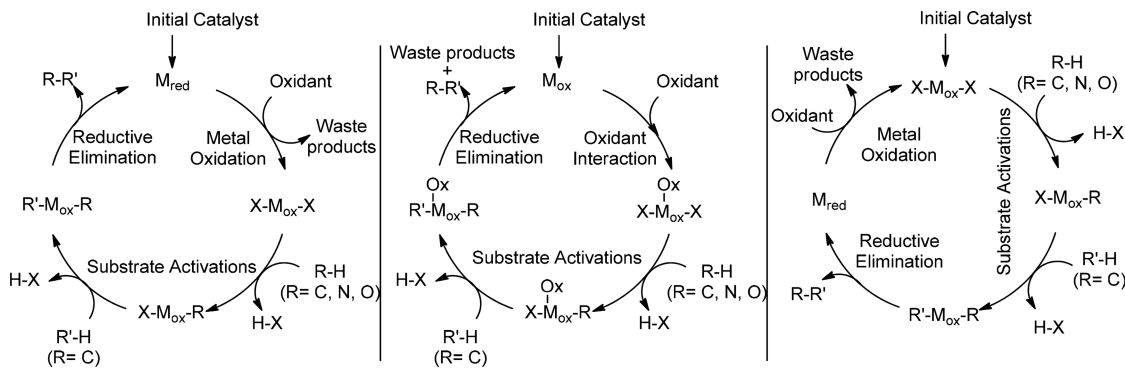
mechanistic studies, and future work is still needed to provide a more general scenario. The catalytic cycles for these oxidants often involve second- or third-row transition-metal catalysts, and the oxidant participates in the reductive elimination step where the product is released. A dramatic example of this effect is the use of internal oxidants, which determine many aspects in the reactivity, such as regioselectivity or even chemoselectivity.

Metal-free oxidants, such as dioxygen, also actively participate throughout the catalytic cycle, facilitating the activation of the substrates and the reductive elimination. They are often combined with first-row transition metals, probably because these processes are prone to the involvement of single electron transfer steps. According to all this information, three different catalytic cycles can be proposed, depending on the role of the oxidant (see Scheme 5).

The first option occurs when the catalyst is activated by the oxidant in the initial stage of the reaction (Scheme 5, left). In this case, the catalyst starts in a reduced inactive state, and the oxidant is needed to form the active species that reacts with the substrates and promotes the coupling. A second option is that of the intimate cooperation between the oxidant and the main catalyst during the cycle (Scheme 5, center).^{102,103} In this case, the oxidant plays a double role, both as a co-catalyst and electron acceptor. A clear example where this catalytic cycle operates is the case of internal oxidants, where they are directly attached to one substrate and therefore, they participate along the entire mechanism. The third option consists of the regeneration of the catalytic cycle once the reaction has been carried out by the main catalyst (Scheme 5, right). This third mechanism, as far as we know, has been the one most often proposed for the oxidative coupling reactions, normally based on stoichiometric reactions carried out without the oxidant. It has a big advantage in its formal simplicity, because it follows the cross-coupling mechanism with only an extra step. However, its generality is questionable, as it can hardly explain the effect of the oxidant in the chemoselectivity or regioselectivity of the process in specific cases.

Some general mechanistic ideas are already coming into focus in this area under development. Oxidative coupling reaction mechanisms are complex and dependent on several factors, such as the main catalyst, the oxidant employed, the solvent, and other additives. DFT calculations have been demonstrated to be a valuable methodology to understand most of the factors in the reactions (i.e., regioselectivity, chemoselectivity, or enantioselectivity). More work is particularly needed on the role of the oxidant in the catalytic cycle.

Scheme 5. Different Catalytic Cycles for Oxidative Coupling Reactions: (Left) Catalyst Activated by the Oxidant, (Center) Cooperative Role of the Oxidant during the Cycle, and (Right) Regeneration of the Catalytic Cycle by the Oxidant



Speciation of metal salts and active species in organic solvent solution is relevant to the mechanistic studies. There is the danger that the application of oversimplified models (i.e., simple molecular ion-pairs) in computational studies can affect the thermodynamics and the kinetics of the reaction; therefore, the issue should be treated carefully in future work in the field.

8. CONCLUSIONS AND OUTLOOK

In this perspective, we have presented the current picture on the mechanism of oxidative coupling that emerges from DFT calculations. This is an evolving field of research which, similar to oxidative coupling itself, is far from settled, but significant progress has been made. Most of the publications so far have focused on a specific step, such as the C–H activation or the selectivity determining step. Their joint consideration, and that of the few works addressing the full catalytic cycle, allow some general ideas to emerge. In our opinion, the need of an oxidative step complicates the mechanistic studies, in comparison with classic cross-coupling reaction; however, at the same time, it is a promising opportunity for computational chemistry, especially in the cooperative cases, where there are many ways to tune the reactivity and predict new reactions. The issue is further complicated because the presence of metal salts as oxidants complicates the description of catalyst speciation in solution, which is still a matter of discussion in the field. The increase in computer power as well as the development of modern density functionals now allows one to calculate real systems and even full catalytic cycles. The inclusion of dispersion forces and the possibility of optimizing the structures in solution, using implicit solvent models, have considerably improved the accuracy of the calculations in the field. However, the presence of open-shell species and the intrinsic problems derived from the complexity of oxidative coupling reactions, because of the effect of additives and electron transfer steps, are still a challenge and require further and more complete studies in the near future. However, the reward to answering these challenges is high, because there are questions remaining with regard to the role of the oxidant, generation of the active species, catalyst regeneration, or reaction selectivity that are still far from being fully understood, and these questions seem to be key to further optimization of the catalytic processes. DFT calculations have been demonstrated to be a valuable tool for the mechanistic study of oxidative coupling, and we are convinced that they will play a relevant role in future developments in the field.

AUTHOR INFORMATION

Corresponding Author

*E-mail: fmaseras@iciq.es.

ORCID

Ignacio Funes-Ardoiz: 0000-0002-5843-9660

Feliu Maseras: 0000-0001-8806-2019

Notes

The authors declare no competing financial interest.

ACKNOWLEDGMENTS

We thank the financial support from the CERCA Programme/Generalitat de Catalunya and MINECO (Project No. CTQ2014-57661-R and Severo Ochoa Excellence Accreditation 2014–2018 SEV-2013-0319). I.F.-A thanks the Severo Ochoa predoctoral training fellowship (Ref. No. SVP-2014-0686662).

REFERENCES

- (1) Nishihara, Y. *Applied Cross-Coupling Reactions*, 1st Edition; Springer-Verlag: Berlin, Germany, 2013.
- (2) *The Nobel Prize in Chemistry 2010*; available via the Internet at: http://www.nobelprize.org/nobel_prizes/chemistry/laureates/2010/; accessed July 21, 2017.
- (3) Li, C.-J. *Handbook of Green Chemistry*, Vol. 7; Wiley-VCH: Weinheim, Germany, 2012.
- (4) Lei, A.; Shi, W.; Liu, C.; Liu, W.; Zhang, H.; He, C. *Oxidative Cross-Coupling Reactions*, 1st Edition; Wiley-VCH: Weinheim, Germany, 2017.
- (5) Moragas, T.; Correa, A.; Martin, R. *Chem.—Eur. J.* **2014**, *20*, 8242–8258.
- (6) Prier, C. K.; Rankic, D. A.; MacMillan, D. W. C. *Chem. Rev.* **2013**, *113*, 5322–5363.
- (7) Romero, N. A.; Nicewicz, D. A. *Chem. Rev.* **2016**, *116*, 10075–10166.
- (8) Fernández-Álvarez, V. M.; Nappi, M.; Melchiorre, P.; Maseras, F. *Org. Lett.* **2015**, *17*, 2676–2679.
- (9) Horn, E. J.; Rosen, B. R.; Baran, P. S. *ACS Cent. Sci.* **2016**, *2*, 302–308.
- (10) Savéant, J.-M. *Chem. Rev.* **2008**, *108*, 2348–2378.
- (11) Funes-Ardoiz, I.; Sameera, W. M. C.; Romero, R. M.; Martínez, C.; Souto, J. A.; Sampedro, D.; Muñoz, K.; Maseras, F. *Chem.—Eur. J.* **2016**, *22*, 7545–7553.
- (12) Braga, A. A. C.; Morgon, N. H.; Ujaque, G.; Maseras, F. *J. Am. Chem. Soc.* **2005**, *127*, 9298–9307.
- (13) García-Melchor, M.; Braga, A. A. C.; Lledós, A.; Ujaque, G.; Maseras, F. *Acc. Chem. Res.* **2013**, *46*, 2626–2634.
- (14) Sperger, T.; Sanhueza, I. A.; Kalvet, I.; Schoenebeck, F. *Chem. Rev.* **2015**, *115*, 9532–9586.
- (15) Xue, L.; Lin, Z. *Chem. Soc. Rev.* **2010**, *39*, 1692–1705.
- (16) Ueura, K.; Satoh, T.; Miura, M. *Org. Lett.* **2007**, *9*, 1407–1409.
- (17) Ueura, K.; Satoh, T.; Miura, M. *J. Org. Chem.* **2007**, *72*, 5362–5367.
- (18) Sameera, W. M. C.; Maseras, F. *WIREs Comput. Mol. Sci.* **2012**, *2*, 375–385.
- (19) Becke, A. D. *J. Chem. Phys.* **1993**, *98*, 5648–5652.
- (20) Stephens, P. J.; Devlin, F. J.; Chabalowski, C. F.; Frisch, M. J. *J. Phys. Chem.* **1994**, *98*, 11623–11627.
- (21) Zhao, Y.; Schultz, N. E.; Truhlar, D. G. *J. Chem. Theory Comput.* **2006**, *2*, 364–382.
- (22) Zhao, Y.; Truhlar, D. G. *J. Chem. Phys.* **2006**, *125*, 194101–18.
- (23) Grimme, S. *J. Comput. Chem.* **2006**, *27*, 1787–1799.
- (24) Grimme, S.; Antony, J.; Ehrlich, S.; Krieg, H. *J. Chem. Phys.* **2010**, *132*, 154104.
- (25) Marenich, A. V.; Cramer, C. J.; Truhlar, D. G. *J. Phys. Chem. B* **2009**, *113*, 6378.
- (26) Yang, Y.; Lan, J.; You, J. *Chem. Rev.* **2017**, *117*, 8787–8863.
- (27) Labinger, J. A.; Bercaw, J. E. *Nature* **2002**, *417*, 507–514.
- (28) Bergman, R. G. *Nature* **2007**, *446*, 391–393.
- (29) Godula, K.; Sames, D. *Science* **2006**, *312*, 67–72.
- (30) Boutadla, Y.; Davies, D. L.; Macgregor, S. A.; Poblador-Bahamonde, A. I. *Dalton Trans.* **2009**, *0*, 5820–5831.
- (31) Balcells, D.; Clot, E.; Eisenstein, O. *Chem. Rev.* **2010**, *110*, 749–823.
- (32) Guan, W.; Sayyed, F. B.; Zeng, G.; Sakaki, S. *Inorg. Chem.* **2014**, *53*, 6444–6457.
- (33) Jiang, Y.-Y.; Man, X.; Bi, S. *Sci. China: Chem.* **2016**, *59*, 1448–1466.
- (34) Jones, W. D. *Inorg. Chem.* **2005**, *44*, 4475–4484.
- (35) Lapointe, D.; Fagnou, K. *Chem. Lett.* **2010**, *39*, 1118–1126.
- (36) García-Cuadrado, D.; Braga, A. A. C.; Maseras, F.; Echavarren, A. M. *J. Am. Chem. Soc.* **2006**, *128*, 1066–1067.
- (37) García-Cuadrado, D.; de Mendoza, P.; Braga, A. A. C.; Maseras, F.; Echavarren, A. M. *J. Am. Chem. Soc.* **2007**, *129*, 6880–6886.
- (38) Davies, D. L.; Macgregor, S. A.; McMullin, C. L. *Chem. Rev.* **2017**, *117*, 8649–8709.
- (39) Satoh, T.; Miura, M. *Chem.—Eur. J.* **2010**, *16*, 11212–11222.

- (40) Colby, D. A.; Tsai, A. S.; Bergman, R. G.; Ellman, J. A. *Acc. Chem. Res.* **2012**, *45*, 814–825.
- (41) Song, G.; Wang, F.; Li, X. *Chem. Soc. Rev.* **2012**, *41*, 3651–3678.
- (42) Patureau, F. W.; Wencel-Delord, J.; Glorius, F. *Aldrichimica Acta* **2012**, *45*, 31–41.
- (43) Lyons, T. W.; Sanford, M. S. *Chem. Rev.* **2010**, *110*, 1147–1169.
- (44) Le Bras, J.; Muzart, J. *Chem. Rev.* **2011**, *111*, 1170–1214.
- (45) Arockiam, P. B.; Bruneau, C.; Dixneuf, P. H. *Chem. Rev.* **2012**, *112*, 5879–5918.
- (46) Ackermann, L. *Acc. Chem. Res.* **2014**, *47*, 281–295.
- (47) Moselage, M.; Li, J.; Ackermann, L. *ACS Catal.* **2016**, *6*, 498–525.
- (48) Guo, X.-X.; Gu, D.-W.; Wu, Z.; Zhang, W. *Chem. Rev.* **2015**, *115*, 1622–1651.
- (49) Stuart, D. R.; Fagnou, K. *Science* **2007**, *316*, 1172–1175.
- (50) Fukutani, T.; Umeda, N.; Hirano, K.; Satoh, T.; Miura, M. *Chem. Commun.* **2009**, 5141–5143.
- (51) Louillat, M.-L.; Biafora, A.; Legros, F.; Patureau, F. W. *Angew. Chem., Int. Ed.* **2014**, *53*, 3505–3509.
- (52) Zheng, J.; Wang, S.-B.; Zheng, C.; You, S.-L. *J. Am. Chem. Soc.* **2015**, *137*, 4880–4883.
- (53) Ruiz, S.; Villuendas, P.; Ortuño, M. A.; Lledós, A.; Urriolabeitia, E. P. *Chem.—Eur. J.* **2015**, *21*, 8626–8636.
- (54) Du, Y.; Hyster, T. K.; Rovis, T. *Chem. Commun.* **2011**, *47*, 12074–12076.
- (55) Neely, J. M.; Rovis, T. *J. Am. Chem. Soc.* **2013**, *135*, 66–69.
- (56) Liu, B.; Hu, P.; Zhou, X.; Bai, D.; Chang, J.; Li, X. *Org. Lett.* **2017**, *19*, 2086–2089.
- (57) Stephens, D. E.; Lakey-Betitia, J.; Chavez, G.; Ilie, C.; Arman, H. D.; Larionov, O. V. *Chem. Commun.* **2015**, *51*, 9507–9510.
- (58) Stuart, D. R.; Bertrand-Laperle, M.; Burgess, K. M. N.; Fagnou, K. *J. Am. Chem. Soc.* **2008**, *130*, 16474–16475.
- (59) Martínez, A. M.; Echavarren, J.; Alonso, I.; Rodríguez, N.; Gómez Arrayás, R.; Carretero, J. C. *Chem. Sci.* **2015**, *6*, 5802–5814.
- (60) Xi, P.; Yang, F.; Qin, S.; Zhao, D.; Lan, J.; Gao, G.; Hu, C.; You, J. *J. Am. Chem. Soc.* **2010**, *132*, 1822–1824.
- (61) Algarra, A. G.; Cross, W. B.; Davies, D. L.; Khamker, Q.; Macgregor, S. A.; McMullin, C. L.; Singh, K. *J. Org. Chem.* **2014**, *79*, 1954–1970.
- (62) Davies, D. L.; Ellul, C. E.; Macgregor, S. A.; McMullin, C. L.; Singh, K. *J. Am. Chem. Soc.* **2015**, *137*, 9659–9669.
- (63) Zheng, C.; Zheng, J.; You, S.-L. *ACS Catal.* **2016**, *6*, 262–271.
- (64) Quiñones, N.; Seoane, A.; García-Fandiño, R.; Mascareñas, J. L.; Gulías, M. *Chem. Sci.* **2013**, *4*, 2874–2879.
- (65) Li, L.; Brennessel, W. W.; Jones, W. D. *Organometallics* **2009**, *28*, 3492–3500.
- (66) Jiang, J.; Ramozzi, R.; Morokuma, J. *Chem.—Eur. J.* **2015**, *21*, 11158–11164.
- (67) Tsybizova, A.; Ryland, B. L.; Tsierkezos, N.; Stahl, S. S.; Roithová, J.; Schröder, D. *Eur. J. Inorg. Chem.* **2014**, *2014*, 1407–1412.
- (68) Funes-Ardoiz, I.; Maseras, F. *Angew. Chem., Int. Ed.* **2016**, *55*, 2764–2767.
- (69) Choi, H.; Min, M.; Peng, Q.; Kang, D.; Paton, R. S.; Hong, S. *Chem. Sci.* **2016**, *7*, 3900–3909.
- (70) Ishikawa, A.; Nakao, Y.; Sato, H.; Sakaki, S. *Dalton Trans.* **2010**, *39*, 3279–3289.
- (71) Yang, Y.-F.; Cheng, G.-J.; Liu, P.; Leow, D.; Sun, T.-Y.; Chen, P.; Zhang, X.; Yu, J.-Q.; Wu, Y.-D.; Houk, K. N. *J. Am. Chem. Soc.* **2014**, *136*, 344–355.
- (72) Frasco, D. A.; Lilly, C. P.; Boyle, P. D.; Ison, E. A. *ACS Catal.* **2013**, *3*, 2421–2429.
- (73) Gao, B.; Liu, S.; Lan, Yu; Huang, H. *Organometallics* **2016**, *35*, 1480–1487.
- (74) Leitch, J. A.; Wilson, P. B.; McMullin, C. L.; Mahon, M. F.; Bhonoah, Y.; Williams, I. H.; Frost, C. G. *ACS Catal.* **2016**, *6*, 5520–5529.
- (75) Guimond, N.; Gorelsky, S. I.; Fagnou, K. *J. Am. Chem. Soc.* **2011**, *133*, 6449–6457.
- (76) Semakul, N.; Jackson, K. E.; Paton, R. S.; Rovis, T. *Chem. Sci.* **2017**, *8*, 1015–1020.
- (77) Neufeldt, S. R.; Jiménez-Osés, G.; Huckins, J. R.; Thiel, O. R.; Houk, K. N. *J. Am. Chem. Soc.* **2015**, *137*, 9843–9854.
- (78) Xu, L.; Zhu, Q.; Huang, G.; Cheng, B.; Xia, Y. *J. Org. Chem.* **2012**, *77*, 3017–3024.
- (79) Anand, M.; Sunoj, R. B.; Schaefer, H. F. *J. Am. Chem. Soc.* **2014**, *136*, 5535–5538.
- (80) Anand, M.; Sunoj, R. B.; Schaefer, H. F. *ACS Catal.* **2016**, *6*, 696–708.
- (81) Yi, H.; Zhang, G.; Wang, H.; Huang, Z.; Wang, J.; Singh, A. K.; Lei, A. *Chem. Rev.* **2017**, *117*, 9016–9085.
- (82) Zhang, G.; Yang, L.; Wang, Y.; Xie, Y.; Huang, H. *J. Am. Chem. Soc.* **2013**, *135*, 8850–8853.
- (83) Warratz, S.; Kornhaab, C.; Cajaraville, A.; Niepötter, B.; Stalke, D.; Ackermann, L. *Angew. Chem., Int. Ed.* **2015**, *54*, 5513–5517.
- (84) Allen, S. E.; Walvoord, R. R.; Padilla-Salinas, R.; Kozlowski, M. C. *Chem. Rev.* **2013**, *113*, 6234–6458.
- (85) Zhou, L.; Yi, H.; Zhu, L.; Qi, X.; Jiang, H.; Liu, C.; Feng, Y.; Lan, Y.; Lei, A. *Sci. Rep.* **2015**, *5*, 15934–12.
- (86) Zhou, L.; Tang, S.; Qi, X.; Lin, C.; Liu, K.; Liu, C.; Lan, Y.; Lei, A. *Org. Lett.* **2014**, *16*, 3404–3407.
- (87) Xu, Z.-Y.; Jiang, Y.-Y.; Yu, H.-Z.; Fu, Y. *Chem.—Asian J.* **2015**, *10*, 2479–2483.
- (88) Zhang, L.-L.; Li, S.-J.; Zhang, L.; Fang, D.-C. *Org. Biomol. Chem.* **2016**, *14*, 4426–4435.
- (89) Qiu, Y.; Yang, B.; Zhu, C.; Bäckvall, J.-E. *Angew. Chem., Int. Ed.* **2016**, *55*, 6520–6524.
- (90) Babu, B. P.; Meng, X.; Bäckvall, J.-E. *Chem.—Eur. J.* **2013**, *19*, 4140–4145.
- (91) Zheng, X.-W.; Nie, L.; Li, Y.-P.; Liu, S.-J.; Zhao, F.-Y.; Zhang, X.-Y.; Wang, X.-D.; Liu, T. *RSC Adv.* **2017**, *7*, 5013–2017.
- (92) Han, L.; Liu, T. *Org. Biomol. Chem.* **2017**, *15*, 5055–5061.
- (93) Sanhueza, I. A.; Wagner, A. M.; Sanford, M. S.; Schoenebeck, F. *Chem. Sci.* **2013**, *4*, 2767–2775.
- (94) Zhang, S.; Shi, L.; Ding, Y. *J. Am. Chem. Soc.* **2011**, *133*, 20218–20229.
- (95) Hay, A. S. *J. Org. Chem.* **1962**, *27*, 3320–3321.
- (96) Fomina, L.; Vazquez, B.; Tkatchouk, E.; Fomine, S. *Tetrahedron* **2002**, *58*, 6741–6747.
- (97) Jover, J.; Spuhler, P.; Zhao, L.; McArdle, C.; Maseras, F. *Catal. Sci. Technol.* **2014**, *4*, 4200–4209.
- (98) Ranjit, S.; Lee, R.; Heryadi, D.; Shen, C.; Wu, J.; Zhang, P.; Huang, K.-W.; Liu, X. *J. Org. Chem.* **2011**, *76*, 8999–9007.
- (99) Dang, Y.; Deng, X.; Guo, J.; Song, C.; Hu, W.; Wang, Z.-X. *J. Am. Chem. Soc.* **2016**, *138*, 2712–2723.
- (100) Zhang, S.; Chen, Z.; Qin, S.; Lou, C.; Senan, A. M.; Liao, R.-Z.; Yin, G. *Org. Biomol. Chem.* **2016**, *14*, 4146–4157.
- (101) Mei, R.; Wang, H.; Warratz, S.; Macgregor, S. A.; Ackermann, L. *Chem.—Eur. J.* **2016**, *22*, 6759–6763.
- (102) Louillat, M.-L.; Patureau, F. W. *Org. Lett.* **2013**, *15*, 164–167.
- (103) Han, Y.-F.; Jin, G.-X. *Chem. Soc. Rev.* **2014**, *43*, 2799–2823.